Journal of Thermal Analysis, Vol. 38 (1992) 1447-1462

THERMAL ANALYSIS OF OXIDE-ISOLATED STRIPE DIODE LASERS

R.P. Sarzala and W. Nakwaski

INSTITUTE OF PHYSICS, TECHNICAL UNIVERSITY OF LODZ, UL. WOLCZANSKA 219, 93-005 LODZ, POLAND

(Received May 29, 1991)

The finite-element thermal model of the oxide-isolated stripe geometry diode laser is presented in this work. The calculation procedure was carried out with a standard IBM PC/AT microcomputer. The ohmic contact heat generation and the thickness d_{ox} of the SiO_2 layer, as two parameters of OIS lasers crucial from a thermal aspect, were taken into account. The system of isotherms obtained for this laser allowed a discussion of the heat spreading process within the laser structure and a comparison of the relative contributions of all heat sources.

Keywords: oxide-isolated stripe (OIS) diode lasers

Introduction

The operation characteristics of diode lasers are distinctly temperature-dependent. A thermal analysis of their structures is therefore of prime importance.

All the known experimental methods of temperature distribution measurements do not ensure the required accuracy and space resolution. On the other hand, analytical theoretical methods need some simplifying approximations which may limit the accuracy of the results.

An assessment of the usability of a modern numerical method, the finite-element technique, for the thermal analysis of stripe-geometry diode lasers was carried out in [1]. This technique appears to be very exact and surprisingly quick, even when a standard IBM PC/AT microcomputer is used.

The aim of this paper is to carry out a finite-element thermal analysis of the oxide-isolated stripe (OIS) GaAs/(AlGa)As diode laser [2–7]. This structure is still one of the most popular and often used diode laser structures, because of its reliability and relatively simple mass manufacture.

John Wiley & Sons, Limited, Chichester
Akadémiai Kiadó, Budapest

Assumptions

A typical construction of the OIS diode laser is schematically shown in Fig. 1, where the thicknesses of the semiconductor layers and their thermal conductivities [8–11] are also given. The contacting system of the laser is depicted in Fig. 2. The thermal conductivities of the metallic layers have been taken from [12].

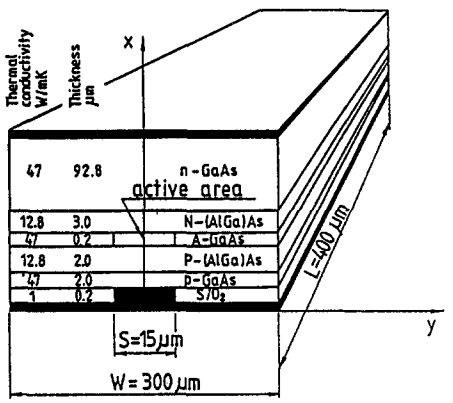

Fig. 1 The oxide-isolated stripe (OIS) double-heterostructure (DH) GaAs-(AlGa)As diode laser. Not to scale. A – active layer, L and W – length and width of the laser crystal, S – stripe width. The coordinate system is also shown.

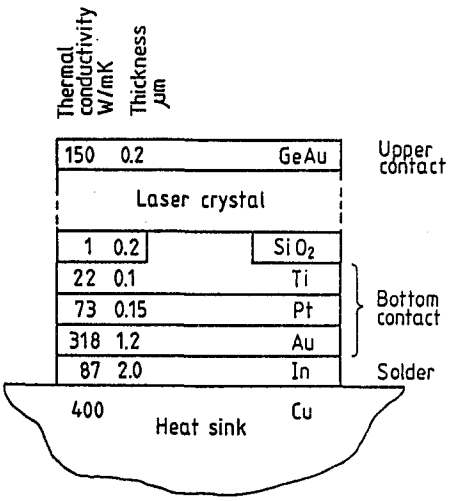

Fig. 2 Contacts of the DH stripe laser under consideration. Not to scale.

The laser is assumed to be supplied with current I = 1 A, much higher than its threshold current I_{TH} = 100 mA. All numerical parameters used in the calculations are listed in Table 1 and shown in Fig.1.

Table 1 Nominal set of the parameters used for temperature calculations for the oxide-isolated stripe DH GaAs-(AlGa)As diode laser

Parameter	Symbol	Value
Ambient temperature	T_A	300 K
Supply current	I	1 A
Threshold current	I_{TH}	100 mA
Voltage drop at the p-n junction	U	1.43 V
Quantum efficiencies:		
– internal, spontaneous emission	a_{sp}	0.55
– internal, lasing	a_i	1
– differential external, lasing	a_E	0.3
The AlAs content difference between the passive and active layers	Δx	0.3
Thickness of the absorbing part of the substrate	d'_N	4 μm
Specific contact resistivity	r	$10^{-5}\ \Omega\ cm^2$

Additionally, the ohmic contact heat generation is taken into account. Its role may be considerable [16, 17], especially in the case of the high excitation considered in this present work, because the Joule heating is proportional to the square of the current density. In accordance with [17], the specific contact resistivity is assumed to be equal to $10^{-5}\ \Omega\ cm^2$. These two p-side surface heat sources are transformed into two volume heat sources inside very thin contact layers, i.e. the GeAu layer and the Ti layer.

Finite-element thermal analysis of the OIS diode laser

Heat sources

The main heat source in diode lasers is located in their active areas as a result of nonradiative recombination and partly the reabsorption of radiation. Its heat generation rate may be expressed [13] as

$$g_A = \frac{U}{d}\left\{j_{TH}(1 - f a_{sp}) + (j - j_{TH})\left[1 - a_E - (1 - a_i)\, a_{sp} f\right]\right\} \tag{1}$$

where d is the active layer thickness, U is the voltage drop at the p-n junction, j and j_{TH} are the supply current density and the threshold current density, respectively, and a_{sp}, a_E and a_i are the internal quantum efficiency of spontaneous emission, the external differential quantum efficiency of lasing and the internal quantum efficiency of lasing, respectively. Coefficient f describes the fraction of spontaneous emission from the active region which is transferred radiatively through the wide-gap passive (AlGa)As layers. This coefficient may be expressed as follows [14]:

$$f = 2\sin^2\left[\frac{1}{2}\arcsin(1 - 0.62\,\Delta x / n_R)\right] \tag{2}$$

where $n_R = 3.59$ [15] is the refractive index of the active region and Δx is the difference step in AlAs content between the passive and the active layers.

The above-mentioned spontaneous radiation which is transferred through the passive layers is absorbed in the capping p-GaAs layer and in the lower part (let us say the layer of thickness d'_N) of the substrate. The corresponding heat generation rates are equal to

$$g_{TR,p} = U j_{TH}\, a_{sp} f / (2 d_p) \tag{3}$$

$$g_{TR,N} = U j_{TH}\, a_{sp} f / (2 d'_N) \tag{4}$$

where d_p is the p-GaAs layer thickness.

The Joule heating is generated in each layer with density

$$g_{J,i} = j^2 \rho_i \tag{5}$$

where ρ_i is the electrical resistivity of the i-th layer. The Joule heating within metal layers is neglected because the heat generation rates are insignificant. Doping concentrations and values of the electrical resistivity of semiconductor layers are listed in Table 2.

All heat generation rates considered in our thermal model of the OIS laser are listed in Table 3 for extremely high excitation (I = 1 A) and for the laser threshold

($I = I_{TH} = 100$ mA). In both cases, the heat source in the active area appears to be the most efficient one. Joule heating generation also plays a surprisingly important role in this process in the case of high excitation, whereas its importance is practically insignificant for the laser threshold. This is the case because the generation rates are proportional to the square of the current density. The heat generation caused by the absorption of spontaneous radiation outside the active area is (for $j \geq j_{TH}$) independent of the supply current, and its influence, high for low supply currents, is therefore gradually reduced with increasing excitation level of a laser.

Table 2 Values of doping concentrations and electrical resistivities of semiconductor layers and contact layers considered in the model

Layer	Doping/10^{18} cm^{-3}	Electrical resistivity/ 10^{-4} Ωm
N – $Al_{0.3}Ga_{0.7}As$	0.12	4.12
P – $Al_{0.3}Ga_{0.7}As$	65.00	0.72
p – GaAs	2.00	2.02
Ti (transformed values)	—	33.33
GeAu (transformed values)	—	50.00

Table 3 Heat generation rates g and heat powers P of individual heat sources in the considered oxide-isolated stripe diode lasers supplied with the currents $I = 1$ A and $I = 100$ mA

Mechanism	Place	P/ mW	g/ 10^{12}Wm^{-3}	Relative particip/ %
Nonradiative recombination and reabsorption of radiation	Active area	825.2 74.4	990.2 89.3	65.3 60.3
Absorption of spontaneous radiation transferred radiatively through passive layers	p – GaAs	2.2 2.2	27.0 27.0	1.8 18.2
	lower part of the substrate	1.1 1.1	27.0 27.0	1.8 18.2
Joule heating	n – GaAs	5.6 0.06	67.2 0.7	4.4 0.5
	N – (AlGa)As	11.4 0.11	205.2 2.1	13.5 1.4
	P – (AlGa)As	2.0 0.02	24.0 0.2	1.6 0.2
	GeAu	0.35 0.003	8.3 0.1	0.6 0.1
	Ti	92.6 0.93	166.7 1.7	11.0 1.1

Current spreading

For diode lasers with relatively small lateral diffusion of carriers [18], the current density distribution at the *p-n* junction is given by [19, 20]

$$j(y) = \begin{cases} j_1 & \text{for } |y| \leq S/2 \\ j_1 / \{[1 + (y - S/2)/l_o]^2\} & \text{for } |y| \leq S/2 \end{cases} \tag{6}$$

with

$$j_1 = j + 2(B/S)^2 - 2(B/S)\,[(B/S)^2 + j\,]^{1/2} \tag{7}$$

$$j = I/(LS) \tag{8}$$

$$l_o = B j_1^{-1/2} \tag{9}$$

$$B = [2n_c\, kT / (Re)] \tag{10}$$

where I is the supply current, S is the stripe width, L is the resonator length, R is the composite sheet resistance in the y direction (cf. the coordinate system in Fig. 1):

$$R^{-1} = \sum_i (d_i / \rho_i) \tag{11}$$

d_i is the thickness of the i-th layer, ρ_i is its electrical resistivity, the summation in (11) is carried out over all layers between the stripe contact and the active area, k is the Boltzmann constant, e is the unit charge and n_c is a constant (for DH GaAs/(AlGa)As diode lasers [21], $n_c = 2$).

We assume the relative distribution of the active area heat generation rate to be the same as for the *p-n* junction current density:

$$g_A(y) = g_A j(y)/j \tag{12}$$

Heat sinking analysis

The spreading thermal resistance Θ_{HS} of the heat sink may be expressed [22] as

$$\Theta_{HS} = [0.5 + \ln(2L / S_{EF})] / (\lambda_{HS}\, \pi L) \tag{13}$$

where λ_{HS} is the heat sink thermal conductivity (for copper, $\lambda_{HS} = 400$ W/mK [12]). Because of the collimating influence of the oxide barriers on the heat flux spreading, the effective width S_{EF} is assumed to be equal to the stripe width S.

The temperature increase ΔT_{HS} within the heat sink is given by

$$\Delta T_{HS} = P_{\Sigma}\,\Theta_{HS} \tag{14}$$

where P_{Σ} is the total dissipated power, which may be expressed as

$$P_{\Sigma} = U\,[I_{TH} + (I - I_{TH})\,(1 - a_E)] + I^2 R_S \tag{15}$$

with R_S being the series electrical resistance of the laser, $R_S = R_{S,S} + R_{S,C}$, $R_{S,S}$ is the series resistance of semiconductor layers, and $R_{S,C}$ is the contact resistance. For the construction under consideration:

$R_S = 0.306\,\Omega$, $R_{S,S} = 0.131\,\Omega$, $R_{S,C} = 0.175\,\Omega$, $P_{\Sigma} = 1.35\,W$

$S_{EF} = S = 15\,\mu m$, $\Theta_{HS} = 8.91\,K/W$, $\Delta T_{HS} = 12.0\,deg$

In the determination of the resistance $R_{S,S}$, two-dimensional current spreading has been taken into account in a simple way.

The finite-element thermal modelling

The perpendicular grid used for the temperature calculations within the GaAs/(AlGa)As OIS diode laser is shown in Fig. 3. Half of the laser structure is divided into $13 \times 38 = 494$ elements. The CPU time for one set of input data amounts to 134 sec when the IBM PC/AT (6 MHz) microcomputer is used.

Isotherms

A system of isotherms for the structure under consideration is shown in Fig. 4. It can be seen that in this case the highest temperature increase, ΔT_{max}, takes place within the active area and amounts to as much as 30.3 deg.

The isotherm configuration allows the evaluation of relative participations of individual heat paths, i.e. it permits the determination of the shape, direction and relative density of individual heat fluxes. Along the x axis, the density of isotherms in the direction towards the heat sink is as much as four times higher than in the opposite direction. Hence, the corresponding heat fluxes are related to each other in the same ratio. On the other hand, the horizontal temperature gradient inside the active area is also four times lower than that inside the passive layer towards the heat sink, but it should be noted that the thermal conductivity of the former area is much higher than that of the latter one. The curvature of the isotherms in the individual layers determines the lateral heat spreading in these layers. Figure 4 shows that the heat fluxes penetrate into regions relatively far from the active area, but reaching the heat sink through the stripe contact. The isothermal lines in the enlarged neighbourhood of the active area of the OIS laser distinctly show the characteristic curving of the heat fluxes because of the high thermal resistance of the oxide layer beyond the stripe region (cf. Fig. 1). All the

thermal resistance of the oxide layer beyond the stripe region (cf. Fig. 1). All the above facts show in what way the shapes of the isothermal lines permit determination of the heat spreading in the neighbourhood of the active area.

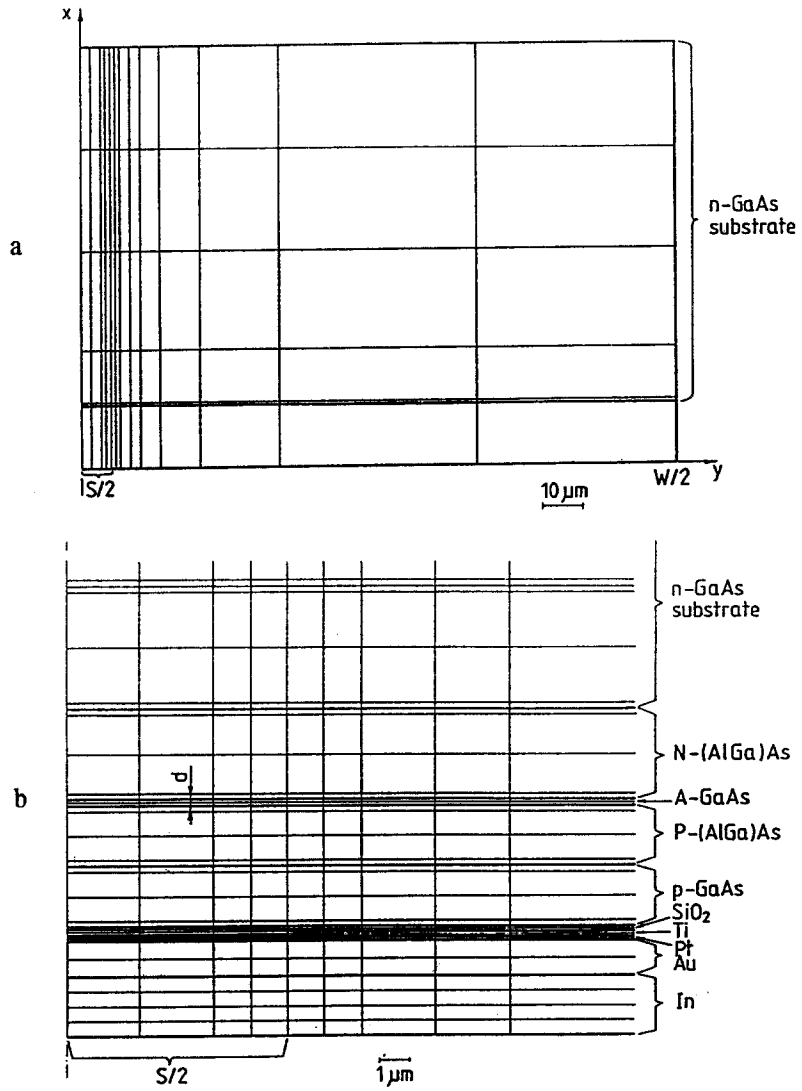

Fig. 3 The perpendicular grid used for the finite-element temperature analysis of the OIS laser: (*a*) whole laser structure, (*b*) an enlarged neighborhood of the active area

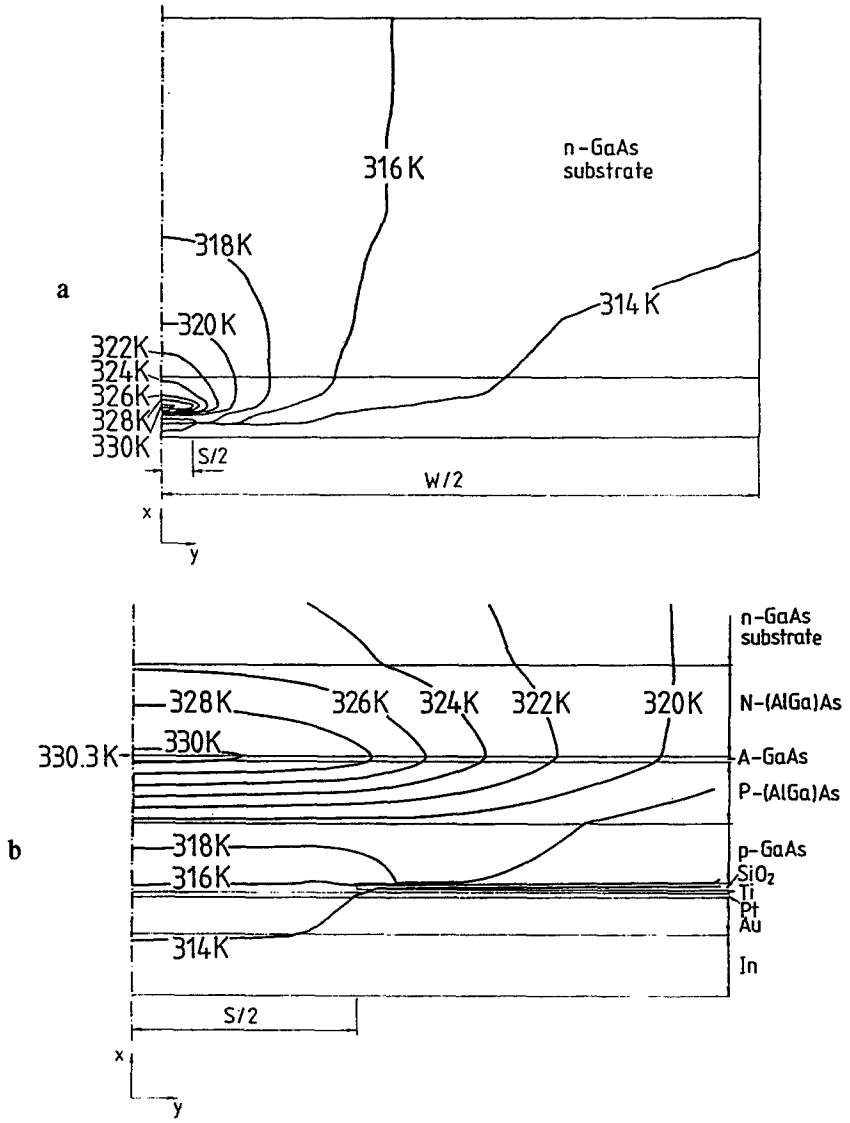

Fig. 4 Isothermal lines in the OIS diode laser: (*a*) whole laser structure, (*b*) an enlarged neighborhood of the active area. In the FEM temperature calculations, the heat-sink temperature increase $\Delta T_{HS} = 12.0$ deg has been taken into account

Temperature profiles

The temperature profile along the x axis is shown in Fig. 5. It can be seen that the temperature changes very quickly within the P-type and the N-type (AlGa)As passive layers. This corresponds to the increasing density of the isotherms observed inside these layers in Fig. 4b [the convex shape of the temperature profile inside the N-type passive layer is a result of its relatively important local heat source [23] (cf. Table 3)].

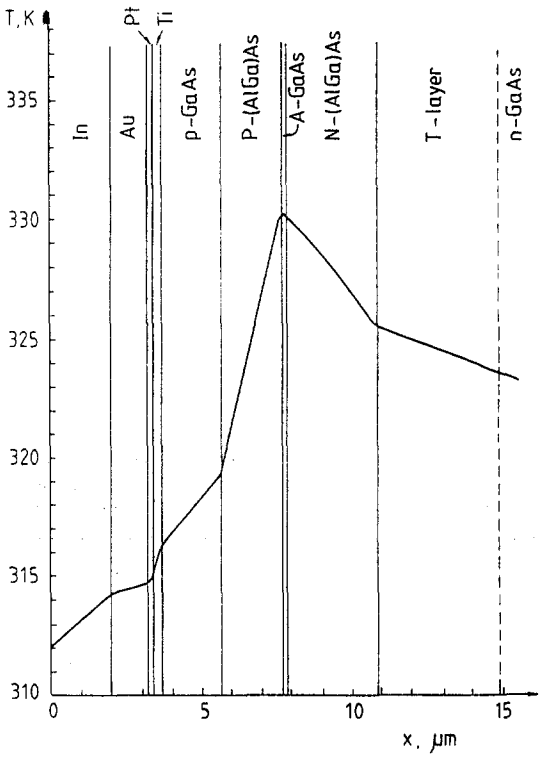

Fig. 5 The temperature profile along the x axis for the OIS diode laser

Horizontal temperature profiles, i.e. along the y axis, in the centres of individual layers are presented in Fig. 6. The temperature gradients in this direction within the (AlGa)As passive layers are slightly lower than those within the active layer, in spite of their much lower thermal conductivity. The temperature gradients in both the high thermal conductivity GaAs layers, i.e. the p-type capping layer, and the lower part of the n-type substrate (T layer), are relatively low. This is evidence of a less important lateral heat spreading mechanism in these layers. On the other hand, in Fig. 6 it can be seen that the temperature gradient within the p-type layer is positive as opposed to other layers. This corresponds to

the opposite curvature of the isotherms observed inside this layer in Fig. 4b. The positive temperature gradient is related to the turning back of the heat fluxes in regions relatively far from the axis of the laser. The heat fluxes penetrate into the heat sink through the stripe region, because beyond the stripe region there is a high thermal resistance oxide layer (cf. Fig. 1).

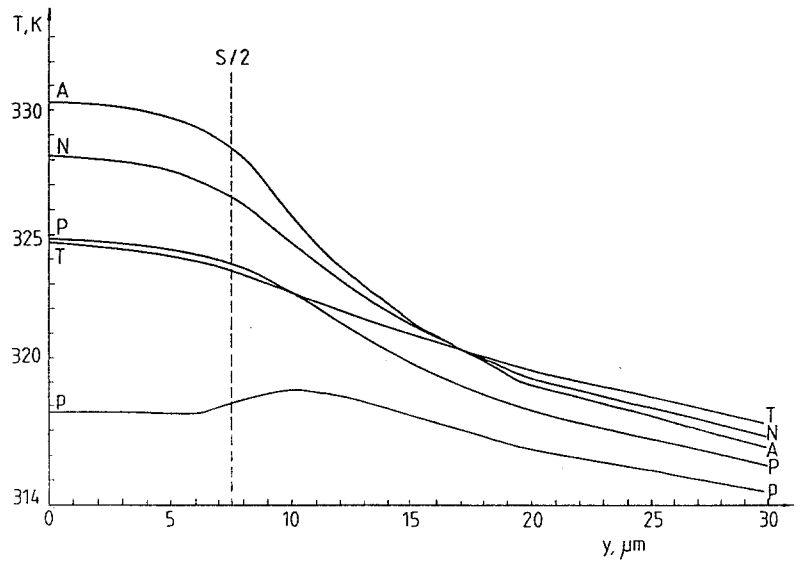

Fig. 6 The temperature profiles along the y axis in the centers of individual layers. A – active layer, N – N-type (AlGa)As layer, P – P-type (AlGa)As layer, p – p-type capping GaAs layer, T – lower part of the substrate absorbing the spontaneous radiation

The thickness d_{ox} of the SiO_2 layer is one of the crucial parameters of OIS lasers from a thermal point of view. Axial temperature profiles for various d_{ox} are shown in Fig. 7. It can be seen that increase of the thickness of the SiO_2 layer by 0.1 μm causes a temperature increase of about 2% within the active area.

Additionally, the ohmic contact heat generation is taken into account in the present work. Axial temperature profiles for various values of contact resistivity for both contact layers, i.e. the GeAu layer and the Ti layer, are shown in Figs 8a and 8b, respectively. Figure 8a demonstrates that the Joule heating generation in the top contact (i.e. in the GeAu layer) has an insignificant effect on the temperature increase which takes place within the diode laser. This is so because the contact is broad and the current density in the layer is relatively small, even for such a high excitation level as considered in the present work (I = 1 A *vs.* I_{TH} = 0.1 A). The situation is different in the bottom contact (i.e. in the Ti layer). This contact is relatively narrow. Therefore, the current density is high in this layer and the

Joule heating generation in the layer causes a high temperature increase within the active area of the diode laser (cf. Fig. 8b).

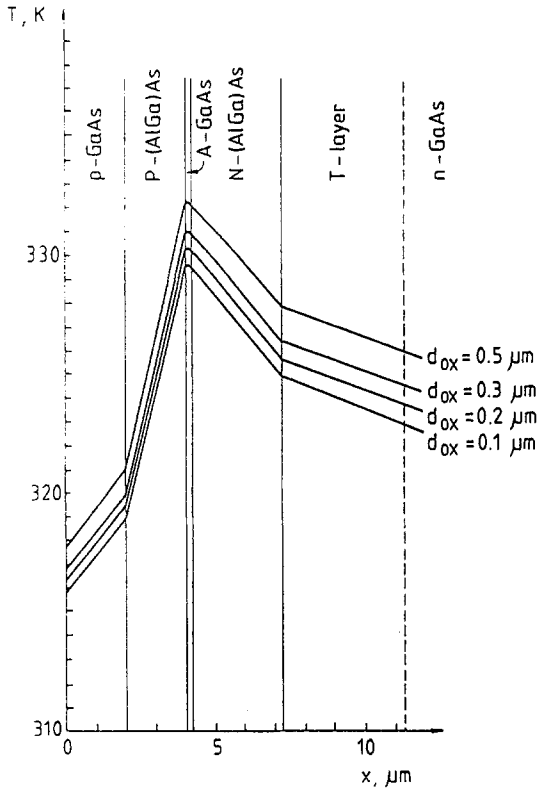

Fig. 7 Axial temperature profiles of the nominal OIS laser with an active area of the dimensions 0.2 μm × 15 μm × 400 μm and supplied with the current 1 A, calculated for various thicknesses d_{ox} of the oxide SiO_2 layer

Both Figs 8a and 8b reveal errors made in the temperature calculations when the ohmic contact heat generation effect is neglected.

The relative participation of the individual heat sources in OIS diode lasers may be discussed on the basis of the plots shown in Fig. 9. It is seen that the Joule heating (especially in the *N*-type (AlGa)As passive layer and the Ti contact layer) makes an important contribution to the overall heating process. However, it should be noted that the Joule heating generation rates are proportional to the second power of the supply current, whereas the remaining rates are proportional only to the first power. Therefore, for such a high excitation level as considered in the present work (I = 1 A *vs.* I_{TH} = 0.1 A), their contribution should be considerable. For lower supply currents, their importance would be less than that of the

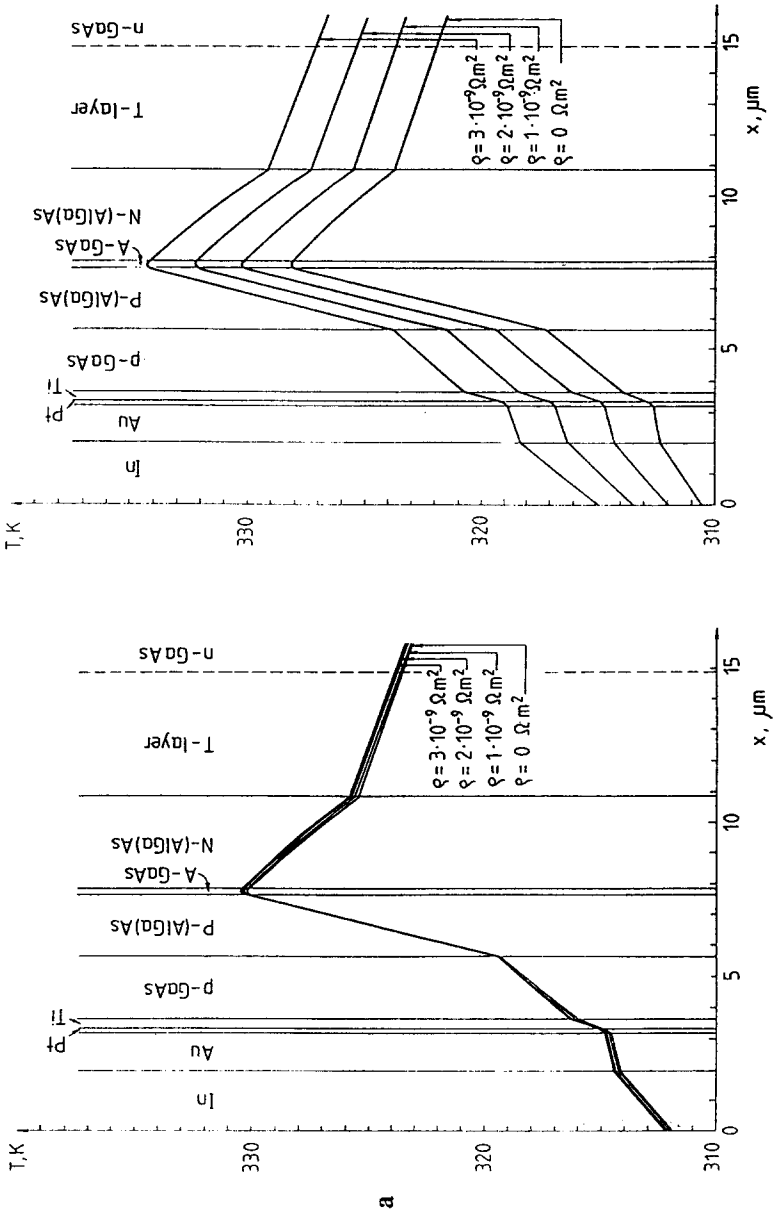

Fig. 8 Axial temperature profiles for various values of contact resistivity: *a*) for top contact layer *i.e.* GeAu layer; *b*) for bottom contact layer *i.e.* Ti layer

heat sources connected with the absorption of spontaneous radiation beyond the active area [24].

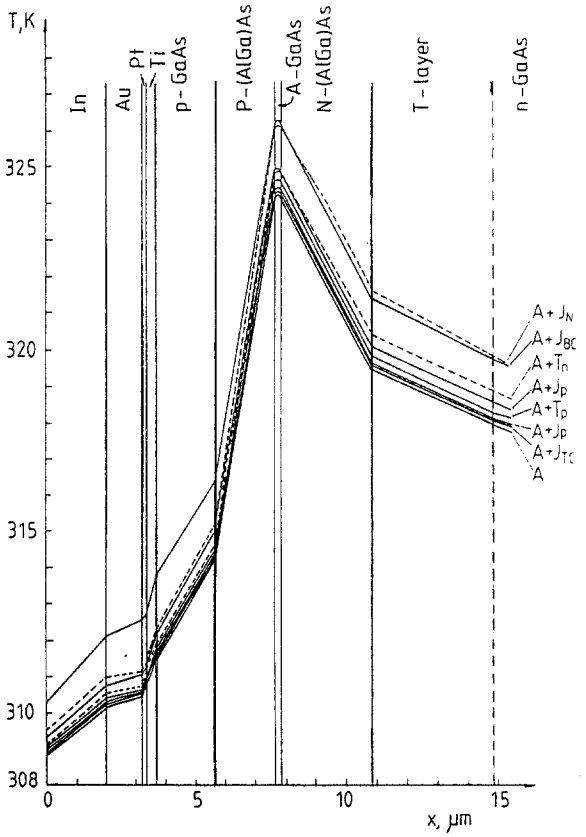

Fig. 9 The temperature profiles along the x axis for various heat sources taken into account; A – active layer heating, J_{TC} – Joule heating in top contact (i.e. in GeAu layer), J_P – Joule heating in the P – type (AlGa)As layer, T_P – absorption of the spontaneous radiation in the p – type GaAs layer, J_p – Joule heating in the p – type GaAs layer, T_n – absorption of the spontaneous radiation in the lower part of the substrate, J_{BC} – Joule heating in bottom contact (i.e. in Ti layer), J_N – Joule heating in the N – type (AlGa)As layer

Conclusions

A finite-element thermal analysis of the oxide-isolated stripe geometry double-heterostructure GaAs/(AlGa)As diode laser has been carried out. This method appears to be very exact and surprisingly quick.

In the case of a standard OIS laser, with active area dimensions $0.2\,\mu m \times 15\,\mu m \times 400\,\mu m$, and an oxide layer thickness $d_{ox} = 0.2\,\mu m$, which is supplied with a current of 1 A, the active area temperature increase is as high as 30.3 deg (including the heat sink temperature increase, $\Delta T_{HS} = 12.0$ deg, and the influence of the bottom contact Joule heating, $\Delta T_{JBC} = 2.0$ deg). The top contact (i.e. the GeAu layer) Joule heating generation may be neglected in the temperature calculations. The thickness d_{OX} of the SiO_2 layer is one of the crucial parameters of OIS lasers from a thermal point of view. The density of the heat flux from the active area directly towards the heat sink appears to be as much as 4 times greater than that in the opposite direction. For such high values of the supply current, the Joule heating plays a considerable role in the overall heating process.

* * *

This work was carried out in program CFRN 117/90 of the Polish Ministry of Education Research project P/04/142/90-2.

References

1 R.P. Sarzala and W. Nakwaski, J. Thermal Anal., 36 (1990) 1171.
2 J.C. Dyment, Appl. Phys. Lett., 10 (1967) 84.
3 J.C. Dyment and L.A. D'Asaro, Appl. Phys. Lett., 11 (1967) 292.
4 J.C. Dyment, J.E. Ripper and T.H. Zachos, J. Appl. Phys., 40 (1969) 1802.
5 J.E. Ripper, J.C. Dyment, L.A. D'Asaro and T.L. Paoli, Appl. Phys. Lett., 18 (1971) 155.
6 C.J. Nuese, Optical Engineering, 18 (1979) 20.
7 M. Ettenberg and H.F. Lockwood, Fiber Integr. Optics, 2 (1979) 47.
8 W. Engeler and M. Garfinkel, Solid-State Electron., 8 (1965) 585.
9 M.A. Afromowitz, J. Appl. Phys., 44 (1973) 1292.
10 S. Adachi, J. Appl. Phys., 54 (1983) 1844.
11 W. Nakwaski, J. Appl. Phys., 64 (1988) 159.
12 D.E. Gray (Ed.), American Institute of Physics Handbook, McGraw-HiII
13 T. Kobayashi and Y. Furukawa, Jpn. J. Appl. Phys., 14 (1975) 1981.
14 W. Nakwaski, Sov. J. Quantum Electron (USA), 9 (1979) 1544 [see also Kvantowaya Elektronika, 6 (1979) 2609 (in Russian)].
15 H.C. Casey Jr., D.D. Sell and M.B. Panish, Appl. Phys. Lett., 24 (1974) 63.
16 J. Piprek and R. Nuernberg, Kvantovaya Elektronika, 15 (1988) 2249 (in Russian).
17 P.A. Morton, M.S. Demokan and R.F. Ormondroyd, submitted to IEE Proceedings, Part J (Optoelectronics).
18 W.B. Joyce, J. Appl. Phys., 51 (1980) 2394.
19 W.B. Joyce and S.H. Wemple, J. Appl. Phys., 41 (1970) 3818.
20 W.B. Dumke, Solid-State Electron., 16 (1973) 1279.
21 C.H. Henry, R.A. Logan and F.R. Merritt, J. Appl. Phys., 49 (1978) 3530.
22 W.B. Joyce and R.W. Dixon, J. Appl. Phys., 46 (1975) 855.
23 W. Nakwaski, Optica Applicata, 13 (1983) 115.
24 W. Nakwaski, IEE Proc.-I (Solid-State and Electron Devices), 131 (1984) 94.

Zusammenfassung — In dieser Arbeit wird ein thermisches Finit-Element-Modell für einen Diodenlaser mit oxid-isolierter Schichtengeometrie vorgestellt. Die mathematischen Berechnungen erfolgten auf einem IBM PC/AT Standard-Microcomputer. Dabei wurden die ohmische Kontaktwärmeentwicklung und die Dicke d_{ox} der SiO_2-Schicht als zwei vom thermischen Gesichtspunkt her ausschlaggebende Parameter für OIS-Laser berücksichtigt. Das für diesen Laser erhaltene System von Isothermen ermöglicht die Diskussion der Wärmestreuungsprozesse innerhalb der Laserstruktur sowie den Vergleich der relativen Beiträge aller Wärmequellen.